

# Effect of Stripes on Electronic States in Underdoped $\text{La}_{2-x}\text{Sr}_x\text{CuO}_4$

T. Tohyama, S. Nagai, Y. Shibata, and S. Maekawa

*Institute for Materials Research, Tohoku University, Sendai 980-8577, Japan*

(Received 4 January 1999)

We investigate the electronic states of underdoped  $\text{La}_{2-x}\text{Sr}_x\text{CuO}_4$  (LSCO) by using a microscopic model, i.e.,  $t$ - $t'$ - $t''$ - $J$  model, containing vertical charge stripes. The numerically exact diagonalization calculation on small clusters shows the consistent explanation of the physical properties in the angle-resolved photoemission, neutron magnetic scattering and optical conductivity experiments such as the antiphase domain and quasi-one-dimensional charge transport. The pair correlation function of the  $d$ -channel is suppressed by the stripes. These results demonstrate a crucial role of the stripes in LSCO

PACS numbers: 74.20.Mn, 71.10.Fd, 74.25.Jb, 74.72.Dn

Since the discovery of high  $T_c$  superconductivity,  $\text{La}_{2-x}\text{Sr}_x\text{CuO}_4$  (LSCO) has been extensively studied as a typical cuprate superconductor, because it has a simple crystal structure with single  $\text{CuO}_2$  layer and the hole density in the  $\text{CuO}_2$  plane is changeable in a wide range from  $x=0$  to 0.35. Understanding of the electronic states of LSCO is, therefore, of crucial importance for the study of the superconductivity.

Recently, Ino *et al.* [1] have performed the angle-resolved photoemission spectroscopy (ARPES) experiment on LSCO and have reported that the spectrum near  $(\pi/2, \pi/2)$  along the  $(0,0)$ - $(\pi, \pi)$  direction is very broad and weak in underdoped samples. The feature is different from the case of underdoped  $\text{Bi}_2\text{Sr}_2\text{CaCu}_2\text{O}_{8+\delta}$  (Bi2212) where a sharp peak appears near  $(\pi/2, \pi/2)$  [2]. The difference between the two typical families may provide a clue of high  $T_c$  superconductivity. Other experimental data in LSCO have also revealed anomalous behaviors of structural [3,4], electronic [5,6] and magnetic properties [7]. In particular, at  $x=0.12$ , an incomplete phase transition from the low temperature orthorhombic (LTO) phase to the low temperature tetragonal (LTT) phase (approximately 10% in volume) has been observed [8]. At the same hole density, the incommensurate antiferromagnetic (AF) long-range order has been reported [9]. It is interesting that the LTT phase of Nd-doped LSCO with  $x=0.12$ ,  $\text{La}_{1.48}\text{Nd}_{0.4}\text{Sr}_{0.12}\text{CuO}_4$ , has shown similar long-range order accompanied by charge order, which is interpreted as charge/spin stripe order that consists of vertical charge stripes and antiphase spin domains [10]. Therefore, such stripes are expected to play an important role in the family of LSCO. From the theoretical side, disorder or fluctuation of the stripe phases has been argued as essential physics of high  $T_c$  superconductors [11–13]. A phenomenological description of the excitation spectrum has also been shown [14].

In this Letter, the electronic states of LSCO are examined in terms of the effect of the stripes on various excitation spectra. We employ a microscopic model with realistic parameters for LSCO (the  $t$ - $J$  model with the

long-range hoppings) under the presence of a potential which stabilizes the vertical stripes, simulating the effect of the LTT fluctuation considered to be favorable for the stripes [3,4]. The numerically exact diagonalization (ED) method is used for small clusters. We find that the vertical stripe formation causes the suppression of the single-particle excitation  $A(\mathbf{k}, \omega)$ , consistent with the ARPES data in underdoped LSCO [1]. This is a direct demonstration that the vertical stripes actually exist in LSCO. The effects of the stripes on other quantities (spin correlation, optical conductivity, and pair correlation) are investigated and the implication of the results is discussed.

The  $t$ - $J$  Hamiltonian with long-range hoppings, termed the  $t$ - $t'$ - $t''$ - $J$  model, is

$$H = J \sum_{\langle i, j \rangle_{1\text{st}}} \mathbf{S}_i \cdot \mathbf{S}_j - t \sum_{\langle i, j \rangle_{1\text{st}} \sigma} c_{i\sigma}^\dagger c_{j\sigma} - t' \sum_{\langle i, j \rangle_{2\text{nd}} \sigma} c_{i\sigma}^\dagger c_{j\sigma} - t'' \sum_{\langle i, j \rangle_{3\text{rd}} \sigma} c_{i\sigma}^\dagger c_{j\sigma} + \text{H.c.}, \quad (1)$$

where the summations  $\langle i, j \rangle_{1\text{st}}$ ,  $\langle i, j \rangle_{2\text{nd}}$  and  $\langle i, j \rangle_{3\text{rd}}$  run over first, second and third nearest-neighbor pairs, respectively. No double occupancy is allowed, and the rest of the notation is standard. Recent analysis of ARPES data has shown that  $t'$  and  $t''$  are necessary for understanding not only the dispersion but also the line shape of the spectral function [2]. In LSCO, we estimated the ratio  $t'/t$  and  $t''/t$  to be  $-0.12$  and  $0.08$ , respectively, by fitting the tight-binding (TB) Fermi surface (FS) to the experimental one in the overdoped sample [1] on the assumption that in the overdoped region the FS shape of the TB band is the same as that of the  $t$ - $t'$ - $t''$ - $J$  model. These numbers are slightly smaller than those for Bi2212,  $t'/t=-0.34$  and  $t''/t=0.23$  ( $t=0.35$  eV) [2]. The contribution of apex oxygen to the band dispersion may be the origin of the difference as discussed by Feiner *et al.* [15]. By performing an ED calculation of  $A(\mathbf{k}, \omega)$  for a 20-site square lattice in the  $t$ - $t'$ - $t''$ - $J$  model, we have confirmed that the quasiparticle (QP) at  $\mathbf{k}=(\pi, 0)$  and  $(0, \pi)$  exists

above the Fermi level in the overdoped region, being consistent with the observed electronlike FS in the highly overdoped sample [1].

In the underdoped region, however, the  $t$ - $t'$ - $t''$ - $J$  results show sharp peaks along the  $(0,0)$ - $(\pi,\pi)$  direction, being inconsistent with the ARPES data [1]. This implies the presence of an additional effect, which may be a stripe formation. It is controversial whether the  $t$ - $J$  model (also  $t$ - $t'$ - $t''$ - $J$  model) itself has the stripe-type ground state (GS) [16–19]. A possible origin of the appearance of stable stripe phase is due to the presence of the long-range part of the Coulomb interaction [20,21] and/or the coupling to lattice distortions. In LSCO, the LTT fluctuation seems to help the latter mechanism [3,4]. In fact, the LTT structure makes Cu-O bonds along  $x$  and  $y$  directions inequivalent, leading to directional distribution of carriers through the anisotropy of the Madelung potential at in-plane oxygen sites and that of the hopping amplitude between Cu-O. To model the directional hole distribution and the tendency toward the stripe instability as simple as possible, we introduce a configuration-dependent “stripe” potential  $V_s$ . The magnitude of  $V_s$  is assumed to depend on the number of holes  $n_h$  in each column along the  $y$  direction of the lattice. In the following, we use a  $\sqrt{18} \times \sqrt{18}$  cluster with two holes as an underdoped system. The maximum number of holes to be considered here amounts to three for the final states of electron removal  $A(\mathbf{k}, \omega)$ . Noting that the 18-site cluster forms three columns under the periodic boundary condition (BC),  $V_s(n_h)$  in each column is assumed that  $V_s(0) = V_s(1) = 0$ ,  $V_s(2) = -2V$ , and  $V_s(3) = -3V$ , being  $V > 0$ . Examples for two configurations are shown in Fig. 1(a).  $V_s(n_h)$  behaves like an attractive potential for holes independent of distance between holes. When the three columns are treated as equivalent, the translational symmetry is preserved and thus the size of the Hilbert space can be reduced. The symmetry with respect to  $90^\circ$  rotation is, however, broken as expected. We note that the present form of  $V_s(n_h)$  is available only for the small cluster with up to three holes [22]. When we treat systems with more than three holes, we need to modify the form of  $V_s(n_h)$  in order to distinguish, for example, between the configurations with a single column filled by four holes and with two columns filled by two holes each.

Let us start on the GS properties of the 18-site cluster with two holes as functions of the potential parameter  $V$ . The total momentum of the GS is always  $(0,0)$ , and a level crossing occurs at  $V/t=0.6$  [23]. For  $0 \leq V/t < 0.6$  the two holes dominantly form a diagonally bounded pair, while for  $V/t > 0.6$  both holes are mainly on a single column with two-lattice spacing. The latter corresponds to the charge stripes expected in LSCO.

Spin correlation around holes in the GS,  $C_s(\alpha, \alpha') \equiv \sum_i \langle \text{GS} | n_i^h \mathbf{S}_{i+\alpha} \cdot \mathbf{S}_{i+\alpha'} | \text{GS} \rangle / N_h$ , is shown in Fig. 1(c). Here  $\alpha$  and  $\alpha'$  denote two sites around a hole following the labeling convention shown in Fig. 1(b).  $n_i^h$  is the hole-

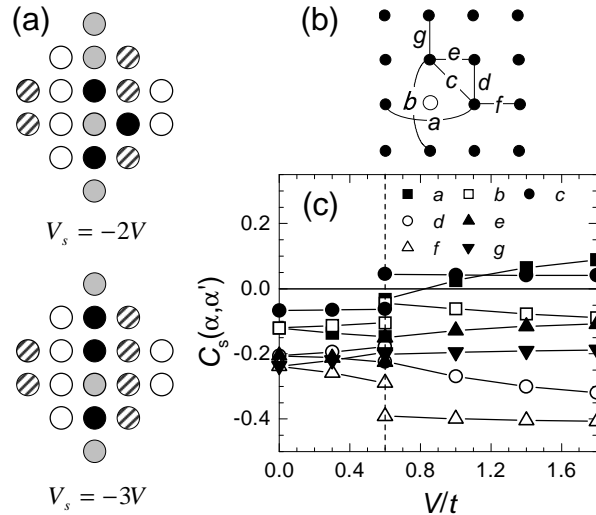


FIG. 1. (a) Illustration of the stripe potential  $V_s$  for the 18-site cluster with periodic BC. The cluster is divided into three columns represented by the empty, shaded and slash circles. When two (three) holes represented by full circles are on a single column,  $V_s = -2V$  ( $-3V$ ). (b) Labeling configurations used for the calculation of spin correlation around holes  $C_s(\alpha, \alpha')$ . The empty circle denotes the position of a hole. (c)  $C_s(\alpha, \alpha')$  of the  $t$ - $t'$ - $t''$ - $J$  model with the stripe potential  $V_s$  on a 18-site 2-hole cluster.  $J/t=0.4$ ,  $t'/t=-0.12$  and  $t''/t=0.08$ . The discontinuity at  $V/t=0.6$  is due to a level crossing.

number operator at site  $i$ , and  $N_h$  is the total number of holes. In the stripe regime ( $V/t > 0.6$ ), the spin correlation for the  $d$  and  $f$  configurations is AF and strong enough to be comparable to the value of  $-0.33$  for the Heisenberg model. The spin correlation in the  $a$  configuration is expected to be AF due to the hole motion [12]. Our result shows sizable AF correlation for  $V/t < 0.6$ . The magnitude is reduced when  $V/t > 0.6$ , since the hole motion perpendicular to the stripes is suppressed. However, the correlation is still AF for  $V/t < 0.8$ . When  $V/t > 0.8$ , it becomes weak ferromagnetic (FM). This FM correlation is, however, due to the periodic BC imposed on the cluster that makes the same spin orientation favorable in the  $a$  configuration. In fact, if we use a  $5 \times 4$  cluster with open BC along the  $x$  direction, the spin correlation across the stripes is always AF with small magnitude ( $\sim -0.05$  for  $V/t=1.0$ ). Such AF correlation is consistent with the experimental observation of the antiphase spin domains [10].

Figure 2 shows the optical conductivity  $\sigma_{||}(\omega)$  and  $\sigma_{\perp}(\omega)$  (parallel and perpendicular to the stripes, respectively) on the 18-site cluster with two holes. When  $V/t=1$ ,  $\sigma_{||}(\omega)$  shows large Drude weight indicating one-dimensional (1D) behavior, whereas the Drude part in  $\sigma_{\perp}(\omega)$  is strongly suppressed. In contrast to ideal 1D systems [24], the sizable incoherent weight remains in  $\sigma_{||}(\omega)$  because the charge carriers in the stripes are not completely free from the spin configuration in the spin

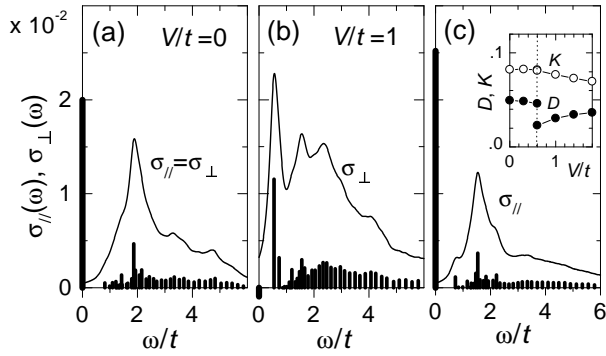


FIG. 2. Optical conductivity,  $\sigma_{\perp}(\omega)$  and  $\sigma_{\parallel}(\omega)$ , of the  $t$ - $t'$ - $t''$ - $J$  model with the stripe potential on a 18-site 2-hole cluster.  $J/t=0.4$ ,  $t'/t=-0.12$  and  $t''/t=0.08$ . (a)  $V/t=0$ . (b) and (c)  $V/t=1$ . The delta functions (vertical bars) for  $\omega/t > 0$  are broadened by a Lorentzian with a width of  $0.2t$  (solid curves). The Drude weights are shown by solid bars at  $\omega/t=0$  multiplied by 0.4. The negative Drude weight in (b) is due to finite-size effect of the cluster. The inset of (c) is the Drude weight and integrated conductivity averaged over both the directions as functions of  $V/t$ .

domains. The quasi-1D nature along the stripes may explain an anomalous  $x$  dependence of the integrated  $\sigma(\omega)$  up to 1.2 eV [6]: it increases linearly up to  $x \sim 0.12$  but above  $x \sim 0.12$  the value is saturated. At  $x \sim 0.12$ , the hole density in each stripe is about 0.5. When more holes enter into the stripes, the kinetic energy of carriers along the stripes decreases since the energy has a maximum at the density of 0.5 in the 1D chain with strong correlation. Thus, the integrated  $\sigma_{\parallel}(\omega)$  decreases. Holes introduced into the spin domains, however, increase the integrated value. Therefore, competition between these two effects causes the saturated behavior above  $x > 0.12$  seen in the experiments.

The inset of Fig. 2(c) shows the total Drude weight  $D$  and the integrated conductivity  $K$  averaged over both the directions. We find that the difference  $K - D$ , which represents the magnitude of the incoherent conductivity, for  $V/t=1$  is larger than that for  $V/t=0$ . The large peak at  $\omega/t \sim 0.6$  in Fig. 2(b), whose energy position is sensitive to  $J$ , is the origin of the difference. These results are consistent with the fact that midinfrared absorption at around  $\omega \sim 0.27$  eV ( $\sim 0.7t$ ) in LSCO is enhanced in comparison with the spectra of  $\text{YBa}_2\text{Cu}_3\text{O}_{6.6}$  and  $\text{Bi2212}$  [25]. With further increasing  $V/t$ , the difference  $K - D$  decreases. This behavior may correspond to the suppression of  $\sigma(\omega)$  observed in Nd-doped LSCO [25].

Figure 3 shows  $A(\mathbf{k}, \omega)$  for selected momenta. When there is no potential [Fig. 3(a)], the large QP peaks are clearly seen below and above the Fermi level at  $(\pi/3, \pi/3)$  and  $(2\pi/3, 2\pi/3)$ , respectively. For  $V/t=1$  [Fig. 3(b)], however, there is no distinct QP peak and the spectra become more incoherent. At  $(\pi/3, \pi/3)$ , a peak is seen above the Fermi level. This may be due to the fact that

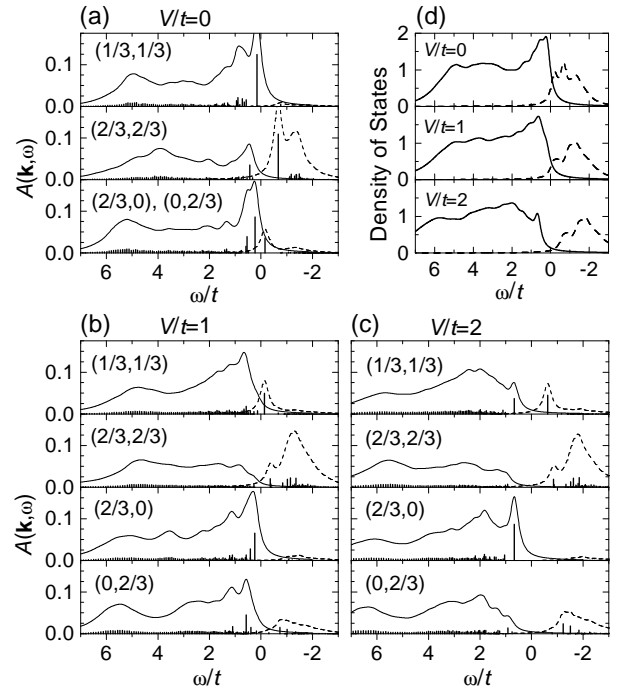


FIG. 3. Single-particle spectral function  $A(\mathbf{k}, \omega)$  of the  $t$ - $t'$ - $t''$ - $J$  model with the stripe potential on a 18-site 2-hole cluster.  $J/t=0.4$ ,  $t'/t=-0.12$  and  $t''/t=0.08$ . (a), (b), and (c) are results for  $V/t=0, 1$ , and  $2$ , respectively. The delta functions (vertical bars) are broadened by a Lorentzian with a width of  $0.2t$  (solid and dashed curves, respectively). The momentum is measured in units of  $\pi$ . (d) The density of states obtained by  $\sum_{\mathbf{k}} A(\mathbf{k}, \omega)$ . The zero energy corresponds to the Fermi level defined as the middle point between the first ionization and affinity states.

the stripe potential behaves like an attractive force between holes. Here, we note that the reduction of QP weight originating from the charge stripes is more or less seen at all momenta. In the presence of the potential, the coupling between charge carriers in the stripes and neighboring spin domains becomes weak (see Fig. 2), and the spin correlation across the stripes is also small [see Fig. 1(c)]. The implication of the two results is an increase of the number of configurations that participate in the GS. According to the configuration interaction picture, such an increase results in the suppression of the QP weight and the increase of incoherent structures. Therefore, the stripe has a general tendency to make the spectrum broad. For  $V/t=2$  [Fig. 3(c)], split-off states from incoherent structures are clearly seen at  $\omega/t=0.7$  for  $(\pi/3, \pi/3)$  and  $(2\pi/3, 0)$ . This is due to the localization of carriers along the direction perpendicular to the stripes [14]. For  $V/t=1$ , the tendency to the localization may be involved in the low-energy peaks at  $(2\pi/3, 0)$ , but can not be recognized at  $(\pi/3, \pi/3)$ . The broadness of the spectrum at  $(\pi/3, \pi/3)$ , i.e., along the  $(0,0)$ - $(\pi, \pi)$  direction, is thus emphasized in contrast to the spectra

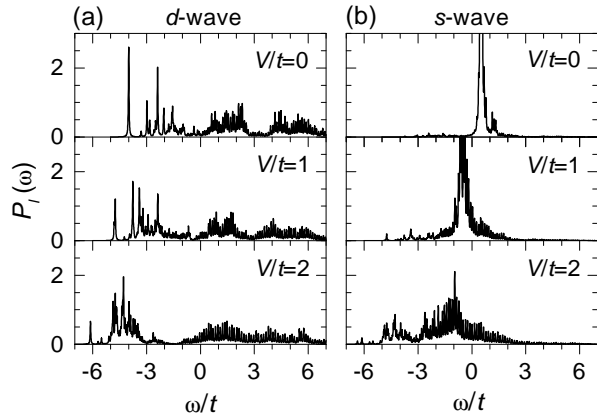


FIG. 4. Two-hole pair spectral function  $P_l(\omega)$  of the  $t$ - $t'$ - $t''$ - $J$  model with the stripe potential on a 18-site 2-hole cluster.  $J/t=0.4$ ,  $t'/t=-0.12$  and  $t''/t=0.08$ . (a)  $d_{x^2-y^2}$ -wave symmetry ( $l=d$ ), and (b)  $s$ -wave symmetry ( $l=s$ ). The delta functions are broadened by a Lorentzian with a width of  $0.02t$ .

for other momenta. As a consequence, our results for  $V/t=1$  explain the ARPES data [1,22]. We also found that the broadness cannot be explained by a diagonal stripe potential. Figure 3(d) illustrates the density of states (DOS). For large  $V/t$ , it shows a gaplike feature near the Fermi level, which may be related to the suppressed DOS at the Fermi level observed in the photoemission experiment [26].

To see the effect of the stripes on the pairing symmetry of carriers, we calculate the pair spectral function  $P_l(\omega)$  for two holes added to the Heisenberg ground state [27], where the hole-pair creation operator is defined by  $N^{-1/2} \sum_{i,\epsilon} \Delta_l(\epsilon) c_{i,\uparrow} c_{i+\epsilon,\downarrow}$  ( $\epsilon$ 's are vectors connecting nearest-neighbor sites) and  $\Delta_l(\epsilon)(=\pm 1)$  depends on  $s$ - or  $d_{x^2-y^2}$ -wave symmetry ( $l=s$  or  $d$ ). For  $V/t=0$ , the low-energy pair fluctuation is dominated by  $d$ -wave symmetry [27] as shown in Fig. 4(a). With increasing  $V$ , the low-energy weight of  $P_d(\omega)$  decreases, while  $P_s(\omega)$  shows enhancement of low-energy fluctuation. This implies that the stripes suppress the  $d$ -wave pairing accompanied by slight enhancement of  $s$ -wave channel [11].

In summary, we have investigated the electronic states of LSCO by using a microscopic model containing the vertical stripes. The tendency toward the formation of vertical charge stripes due to the LTT fluctuation was modeled by the stripe potential, which was added to the  $t$ - $t'$ - $t''$ - $J$  model. The realistic values of  $t'$  and  $t''$  that are smaller than those for Bi2212 were used in the exact diagonalization calculation on small clusters. Here, we comment that the smallness of  $t'$  and  $t''$  also works favorably for the stripe formation [19] as compared with Bi2212. We found that the model explains the ARPES data with suppressed weight along the  $(0,0)$ - $(\pi,\pi)$  direction. Magnetic properties and charge dynamics are consistent with experimental data. The consistent results suggest that the vertical stripe is an essential ingredient for the ex-

planation of the physical properties of LSCO. The pair correlation function of the  $d$ -wave channel is suppressed by the stripes, implying the  $d$ -wave superconductivity is less favorable under the presence of the stripes. This may explain why  $T_c$  in LSCO is so low, as compared with, for example, Bi2212. Our results thus clearly demonstrate the interesting features of the electronic states caused by the stripes, and the uniqueness of LSCO among high  $T_c$  cuprates.

We thank A. Ino, A. Fujimori, S. Uchida and Z.-X. Shen for enlightening discussions. This work was supported by CREST and NEDO. The numerical calculation were performed in the supercomputing facilities in ISSP, Univ. of Tokyo, and IMR, Tohoku Univ.

- 
- [1] A. Ino *et al.*, J. Phys. Soc. Jpn. (to be published), cond-mat/9809311.
  - [2] C. Kim *et al.*, Phys. Rev. Lett. **80**, 4245 (1998).
  - [3] N. L. Saini *et al.*, Phys. Rev. B **55**, 12759 (1997).
  - [4] E. S. Božin *et al.*, Phys. Rev. B **59**, 4445 (1999).
  - [5] A. Ino *et al.*, Phys. Rev. Lett. **79**, 2101 (1997).
  - [6] S. Uchida *et al.*, Phys. Rev. B **43**, 7942 (1991).
  - [7] K. Yamada *et al.*, Phys. Rev. B **57**, 6165 (1998).
  - [8] A. R. Moodenbaugh *et al.*, Phys. Rev. B **58**, 9549 (1998).
  - [9] T. Suzuki *et al.*, Phys. Rev. B **57**, R3229 (1998).
  - [10] J. M. Tranquada *et al.*, Nature (London) **375**, 561 (1995).
  - [11] V. J. Emery *et al.*, Phys. Rev. B **56**, 6120 (1997).
  - [12] J. Zaanen, J. Phys. Chem. Solids **59**, 1769 (1998) and references therein.
  - [13] C. Castellani *et al.*, Phys. Rev. Lett. **75**, 4650 (1995); Physica (Amsterdam) **282-87C**, 260 (1997).
  - [14] M. I. Salkola *et al.*, Phys. Rev. Lett. **77**, 155 (1996).
  - [15] L. F. Feiner *et al.*, Phys. Rev. Lett. **76**, 4939 (1996); R. Raimondi *et al.*, Phys. Rev. B **53**, 8774 (1996).
  - [16] S. R. White and D. J. Scalapino, Phys. Rev. Lett. **80**, 1272 (1998); **81**, 3227 (1998).
  - [17] C. S. Hellberg and E. Manousakis, cond-mat/9812022.
  - [18] K. Kobayashi and H. Yokoyama, Physica (Amsterdam) **259-261B**, 506 (1999).
  - [19] T. Tohyama *et al.*, Phys. Rev. B **59**, R11649 (1999).
  - [20] V. J. Emery and S. A. Kivelson, Physica (Amsterdam) **209C**, 597 (1993).
  - [21] G. Seibold *et al.*, Phys. Rev. B **58**, 13506 (1998).
  - [22] In addition to the 18-site cluster, we have investigated  $4 \times 4$ ,  $4 \times 5$ , and  $5 \times 4$  clusters. The conclusions in the present study depend on neither the size of the clusters nor the details of the form of  $V_s$ , for example, whether the three columns are equivalent or not.
  - [23] At the crossing, the total spin changes from zero to one. By examining different clusters in detail, we found that the change of the total spin is not essential for our results.
  - [24] W. Stephan and P. Horsch, Phys. Rev. B **42**, 8736 (1990).
  - [25] S. Tajima *et al.*, (unpublished); J. Phys. Chem. Solids **59**, 2015 (1998).
  - [26] A. Ino *et al.*, Phys. Rev. Lett. **81**, 2124 (1998).
  - [27] D. Poilblanc, Phys. Rev. B **48**, 3368 (1993).